Molecular Dynamics Simulations of Biotin in Aqueous Solution

Yi Lei, Haoran Li,* Rong Zhang, and Shijun Han

Department of Chemistry, Zhejiang University, Hangzhou, 310027, People's Republic of China

Received: February 20, 2004; In Final Form: April 20, 2004

Molecular dynamics simulations have been used to study the conformational properties and dynamics of biotin in explicit water for the first time. Three simulations, started from different initial conformations, generate similar results, which are characterized in terms of intramolecular distance, radius of gyration, root-mean-square deviation of all atom coordinates, and solvent-accessible surface area. The simulations indicate that biotin in aqueous solution is highly flexible and jumps between extended, semifolded, and folded states. The folded conformations via intramolecular hydrogen bonding are observed. Interestingly, many semifolded biotin molecules involving water-mediated hydrogen bonds between the ureido group and the carboxyl group of the side chain are also observed. The folded and semifolded states of biotin are likely to cause the hydrogen bonding cooperativity, which will activate the 1-NH protons and facilitate the electrophilic substitution of the 1-NH. The flexibility of biotin, the water molecules, and the hydrogen bonding cooperativity may play an essential role in activation of the 1-NH site.

1. Introduction

Biotin serves as a critical enzyme cofactor and participates in carboxylation and carboxyl group transfer reactions.[1−3] As shown in Figure 1, although the two NH protons of biotin, 1-NH and 3-NH protons, are situated at nearly symmetric positions in an ureido ring, only the 1-NH proton is selectively replaced by the carboxyl group. The inherent specificity of biotin in the reversible carboxylation involves the electrophilic substitution of the 1-NH proton by the carboxylate group. The chemical mechanism of carboxylation has attracted considerable speculation, particularly how biotin, a poor nucleophile, is induced to react with bicarbonate, a poor electrophile. For the carboxylation of biotin to occur, biotin must be deprotonated at the 1-N site.[4] Interestingly, isolated biotin and related compounds in solutions also exhibit a certain difference between the 1-NH and 3-NH protons. In addition, the biotin−avidin and biotin−streptavidin bindings are of special interest because they have one of the largest free energies of association yet observed for noncovalent bindings between a protein and a small ligand in aqueous solution.[5,6] Such strong and specific binding between avidin or streptavidin and biotin has led to a wide variety of applications of biotin in immunochemical and diagnostic assays.[7]

Knowledge of the three-dimensional conformations and dynamics of protein-bound and free biotin is important for understanding its biochemical roles and for designing analogues. The spatial structure adopted by a biological molecule is dependent on its environment. While much is known about the structures of protein-bound biotin, the solution structure and dynamics of biotin, especially in water, are less well characterized. The crystal structures of biotin in isolation[8] and bound to a variety of proteins[9] were determined. NMR is often the only method available to study the three-dimensional structure of biochemical molecules in solutions. Fry et al.[10] and Perrin et al.[11] investigated the proton exchange rates in the aqueous solutions by the NMR saturation transfer method and noted that both acid-catalyzed and base-catalyzed proton exchange rates of the 1-NH were 2−4 times faster than those of the 3-NH. This difference was attributed to steric hindrance by the side chain, which reduces the accessibility of the 3-NH. Later, Tonan et al. demonstrated the more rapid rate of exchange for the 1-NH proton compared to the 3-NH proton in biotin by measurements involving the rate of D_2O exchange in dimethyl sulfoxide (DMSO)-d_6.[12] The increased rate of exchange was supposed to form a temporary intramolecular hydrogen bond between the carboxyl group in the valeryl side chain and the 3-NH proton. The NOESY measurements of biotin in DMSO-d_6 further supported the presence of the above conformation. The temperature dependence of the amide proton NMR chemical shift ($\Delta\delta/\Delta T$) has been widely used as a tool for studying intramolecular hydrogen bonding.[13−15] Crisp and Jiang studied the biotin and biotin derivatives in $CDCl_3$ using $\Delta\delta/\Delta T$ and also gave some evidence for intramolecular hydrogen bonding.[16] As known so far, biotin carboxylase required the divalent metal ions Mg^{2+} for the enzymatic reaction.[17] Therefore, Sanchez et al. adopted a macrocyclic magnesium complex and biotin derivatives as model systems and studied the metal−biotin interaction by IR and NMR spectra.[18] Upon addition of the Mg^{2+} complex to a solution of biotin ethyl ester in CD_3CN, the Mg^{2+} complex was found to prefer the binding site of the 1-NH to that of the 3-NH. In addition, Strzelczyk et al. performed a theoretical calculation to find some stable conformations in gas phase, and found that the side chain of biotin could adopt either the extended or folded forms. The folded conformers were stabilized by intramolecular hydrogen bonds.[19]

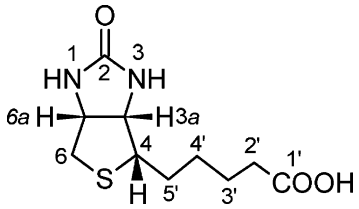

Figure 1. Chemical structure and nomenclature of biotin. The atom types also refer to Table 1.

* Corresponding author. Fax: +86-571-8795-1895. E-mail: lihr@zju.edu.cn.

10.1021/jp049207v CCC: $27.50
Published on Web 06/08/2004

TABLE 1: OPLS-AA Nonbonded Parameters for Biotin

atom	σ (Å)	ϵ (kJ/mol)	q (e)
	Biotin		
N1 (1)	3.250	0.170	−1.0597
H1 (1)	0.000	0.000	0.5177
C2 (ureido)	3.750	0.105	0.8757
O2 (ureido)	2.960	0.210	−0.4484
N3	3.250	0.170	−1.0564
H3	0.000	0.000	0.5164
CT (3a)	3.500	0.066	0.2033
HC (3a)	2.500	0.030	0.1266
CT (6a)	3.500	0.066	0.2014
HC (6a)	2.500	0.030	0.1308
CT (4)	3.500	0.066	−0.1146
HC (4)	2.500	0.030	0.1334
S	3.550	0.250	−0.1714
CT (6)	3.500	0.066	−0.1860
HC1 (6)	2.500	0.030	0.1319
HC2 (6)	2.500	0.030	0.1358
CT (5′)	3.500	0.066	−0.1471
HC1 (5′)	2.500	0.030	0.0936
HC2 (5′)	2.500	0.030	0.1037
CT (4′)	3.500	0.066	−0.1688
HC1 (4′)	2.500	0.030	0.0830
HC2 (4′)	2.500	0.030	0.1026
CT (3′)	3.500	0.066	−0.1612
HC1 (3′)	2.500	0.030	0.1032
HC2 (3′)	2.500	0.030	0.1012
CT (2′)	3.500	0.066	−0.1730
HC1 (2′)	2.500	0.030	0.1220
HC2 (2′)	2.500	0.030	0.1242
C1′ (COOH)	3.750	0.105	0.4128
OH (COOH)	3.000	0.170	−0.5157
O1′ (COOH)	2.960	0.210	−0.4357
HO (COOH)	0.000	0.000	0.4186
	Water		
OW	3.166	0.155	−0.8200
HW	0.000	0.000	0.4100

However, it is not possible to obtain a satisfactory description of the solution conformational space or examination of the balance between the different conformations by the above methods. NMR spectroscopy corresponds to an ensemble and time average over different structures and typically provides structural static pictures. Also, NMR experiments cannot distinguish between different structures coexisting in solution during the time of the measurement. Molecular dynamics (MD) simulation currently offers perhaps the only means of studying at atomic resolution the dynamic equilibrium between the different conformations under realistic conditions. Compared with the "extended" conformation of crystal structure, the previous studies suggested the "folded" conformations in gas phase or in solution, which formed the intramolecular hydrogen bonds between the ureido group and the carboxyl group on the side chain. In the present paper, MD simulations are performed to provide more detailed information about the solution structure and conformational flexibility of biotin in aqueous solution. The information is important to understanding how biotin takes part in the enzymatic carboxylation and carboxyl group transfer reactions. Moreover, the highly complicated heterocyclic and stereochemical structure of biotin is undoubtedly a challenge to MD simulation.

2. Methods

Since so many drug candidates contain heterocyclic rings, recent force field developments have widely expanded to heterocycles. However, the great structural diversity of heterocycles makes it a challenge to classical force fields. As an extension of OPLS all atom (Optimized Potentials for Liquid Simulations All Atom) force field to heterocycles,[20] a new force field of biotin was introduced. Table 1 lists the nonbonded potential parameters and the symbols of atom types. Other potential parameters of biotin are provided in the Supporting Information. The SPC (Single Point Charge) water[21] was used as the water model.

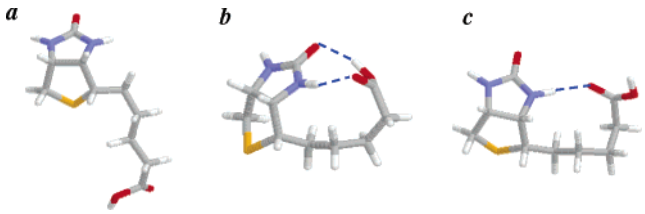

Figure 2. ***a***, conformation of biotin in crystal. ***b***, optimized conformation of most stable folded biotin structure stabilized by two intramolecular hydrogen bonds. ***c***, optimized conformation of sub-stable folded biotin structure stabilized by one intramolecular hydrogen bond. Carbon atoms are shown in gray, nitrogen in blue, oxygen in red, sulfur in yellow, and hydrogen in white.

Classical molecular dynamics simulation of biotin in explicit water was performed using a modified TINKER 4.1 molecular modeling package.[22] A difficult problem remained concerning whether the biotin can reach all native states within a limited simulation time. Therefore, different initial conformations were used to study the whole conformational space and sample conformational space better. One initial structure was taken from the conformation of crystal structure.[8] Based on the crystal structure, the low-energy conformers were further located by performing Monte Carlo calculation, implemented in TINKER 4.1, with the OPLS all atom force field in vacuo. Energy of the preliminary conformers followed to be minimized by a limit memory L-BFGS algorithm with the molecular mechanics calculation. As a result, the two optimized geometries ***b*** and ***c*** were obtained and are shown along with the crystal structure ***a*** in Figure 2. The two conformations of ***b*** and ***c*** were very analogous to those of the quantum chemical calculations in gas phase.[19] The three MD simulations were carried out beginning with the three different conformations of ***a***, ***b***, and ***c***.

The simulations were performed in the NPT ensemble at $P = 1$ atm and $T = 298$ K with periodic boundary condition. The temperature and pressure were maintained with the Berendsen algorithm.[23] The conformer ***a***, ***b***, or ***c*** of biotin was soaked into the center of the 512 water box that had been previously equilibrated. Overlapping water molecules were removed so that the 498, 499, and 501 water molecule boxes remained in the solvent box for simulations 1, 2, and 3, respectively. Then energy minimizations were performed. The equations of motion were integrated with the modified Beeman method.[24] Ewald technique was used to treat the long-range electrostatic interactions.[25] The RATTLE algorithm was used to constrain the bond lengths including hydrogen atoms, while all other degrees of freedom remained flexible.[26] Each system was followed for 6 ns. The first 1 ns was used for equilibration, and the rest of the simulation was used for analysis. Configurations were saved every 0.5 ps.

A simple measure of the conformational flexibility of biotin in aqueous solution was a monitoring of some intramolecular distances as a function of the simulation time. The intramolecular distances between the 3-NH and COOH group were used to describe the conformations and the interactions between the ureido ring and side chain. Both intramolecular and intermolecular hydrogen bonds were decided by the geometric criteria,[27] which were similar to a typical criteria of neat water:

TABLE 2: Calculated Averages and Standard Deviations of MD Simulations

	simulation 1	simulation 2	simulation 3
initial conformation	***a***	***b***	***c***
no. of water molecules	498	499	501
density (g/cm^3)	0.995 ± 0.005	0.994 ± 0.005	0.995 ± 0.005
E_{total} (kcal/mol)	−3967 ± 19	−3969 ± 19	−3988 ± 19
E_{inter} (kcal/mol)	−5264 ± 23	−5268 ± 23	−5292 ± 23
E_{pot} (kcal/mol)	−5022 ± 21	−5026 ± 22	−5049 ± 21
distance[H3···O1′] (Å)	6.76 ± 1.22	6.78 ± 1.23	6.75 ± 1.14
distance[H3···OH] (Å)	7.09 ± 1.30	7.19 ± 1.19	7.17 ± 1.13
radius of gyration (Å)	3.55 ± 0.14	3.56 ± 0.13	3.54 ± 0.15
rmsd (Å)	1.68 ± 0.38	1.72 ± 0.37	1.76 ± 0.34
accessible surface area (Å^2)	446.1 ± 6.8	447.2 ± 5.8	446.0 ± 7.2

R(OW···HW) ≤ 2.40 Å, R(OW···OW) ≤ 3.60 Å, and the angle Φ(HW−OW···OW) ≤ 30°. Radius of gyration (R_g) was defined by

$$R_g = \sqrt{\sum_{i=1}^{N}(r_i - r_g)^2/N}$$

where r_g denotes the position of the centroid of the molecule and r_i denotes the position of the ith atom. Solvent-accessible surface areas of biotin were calculated for a probe radius of 1.4 Å using the algorithm of Connolly.[28] Root-mean-square deviations (rmsd's) of all biotin atom coordinates from conformer ***a*** were also calculated.

3. Results and Discussion

Above all, to understand the biological significances of biotin and water, three fundamental questions need be addressed: (1) Do the folded conformations, which may be relevant for understanding the catalytic mechanism of the enzyme, persist in aqueous solution? (2) Do the biotin solute structures in aqueous solution change significantly from the structures in vacuo, free solid state, and protein-bound solid state? (3) How is the weakly nucleophilic biotin induced to react with bicarbonate, and the 1-NH proton selectively replaced by the carboxyl group in the process of catalysis? Obviously, the first two questions are interrelated and can be solved by recording some time series.

Dynamics and Conformational Analysis. The results of the simulations are summarized in Table 2. The progress of simulation 1 is characterized in terms of intramolecular distance, R_g, rmsd, and solvent-accessible surface area and is shown in Figure 3. Those of simulations 2 and 3 are provided in the Supporting Information. The dynamics of the properties show consistency. The shorter the distances of H3···O1′ or H3···OH are, the more folded conformations. Also, the folded conformations represent small R_g's, accessible surface areas, and large rmsd's. Due to the reductions of the accessible surface areas, the folded biotin molecules will result in decreasing degree of solvation.

The starting structure of simulation 1 is the extended conformer ***a*** observed in the crystal structure. Both simulation 2 and simulation 3 are initiated by the folded biotin conformations ***b*** and ***c***, which present near-spherical molecules stabilized by two intramolecular hydrogen bonds (N3−H3···O1′ and OH−HO···O2) and one intramolecular hydrogen bond (N3−H3···O1′), respectively. However, the intramolecularly hydrogen bonded conformations are rapidly replaced by the hydrogen bonds to the more mobile water molecules, even though the intramolecular donor−acceptor geometry is favorable in vacuo. The dynamics of biotin in aqueous solution are highly flexible. The time series of the intramolecular distances H3···O1′ and H3···OH in Figure 3 clearly illustrate that biotin does not occupy a unique native state in aqueous solution but jumps between extended, semifolded, and folded states. The states of biotin can be classified in terms of the distribution for the square of the radius of gyration. The extended state is classified as the range of conformations where $R_g^2 > 12.0$ Å^2, with the semifolded state for conformations having R_g^2 between 10.5 and 12.0 Å^2 and the folded state for conformations having $R_g^2 < 10.5$ Å^2.

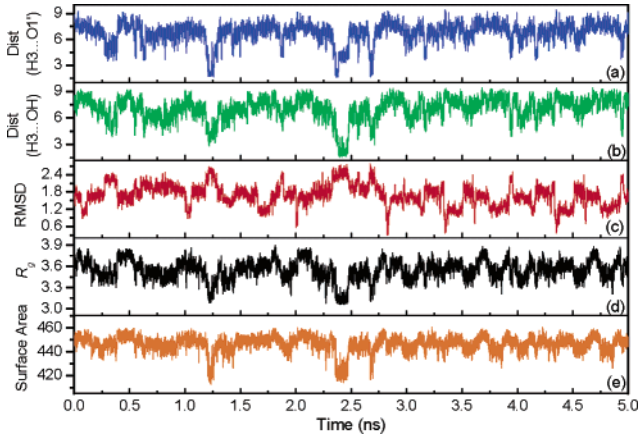

Figure 3. Time series of (a) intramolecular distances H3···O1′ in angstroms (Å), (b) intramolecular distances H3···OH in Å, (c) radius of gyration in Å, (d) rmsd from crystal structure in Å, (e) solvent-accessible surface areas in Å^2 for simulation 1.

In the time series analysis, averages and standard deviations of data are also given in Table 2. The average conformations of the three simulations possessed nearly identical R_g's, rmsd's, intramolecular distances, and solvent-accessible surfaces, which produce the nearly same average conformation of biotin in aqueous solution. Thus, the three simulations, started from different initial conformations, generate similar results. The degree of reproducibility observed here suggests that the 5-ns simulations represented a reasonable degree of conformational sampling. This fact also suggests that the present simulations can describe the structure and dynamics of biotin in aqueous solution with reasonable precision and accuracy. All three simulations observe the folding of forming intramolecular hydrogen bonds and most representative conformations in the 5-ns simulation trajectories. Some representative structures are displayed in Figure 4. The average conformation of simulation 1 is also shown as ***n*** in Figure 4. In the case of simulation 1, the N3−H3···O1′ intramolecularly hydrogen bonded conformations like ***d***, which is very analogous to the initial conformation of ***c***, are observed near 1.23, 2.37, and 2.68 ns, approximately corresponding to the distances of H3···O1′ that are less than 2.4 Å. In addition, the N3−H3···OH intramolecular hydrogen bonded conformations like ***e*** are also observed near 2.42 ns. However the supposed conformation of ***b***,[12,16] the most stable folded one in vacuo, is not observed in the three simulations. The following sections will discuss the three simulations together.

Role of Water. To investigate the role of solvent water in the hydration process, we extract numerous structures of hydrated biotin molecules from the MD trajectories and perform a graphical inspection. Some representative examples of the hydrated biotin are given in Figure 5. Biotin is an amphiphilic molecule. The hydrophilic ureido and carboxyl groups can interact with water to form strong intermolecular hydrogen bonds, or biotin can form intramolecular hydrogen bonds by folding over on itself. Other hydrophobic sites can cause effects

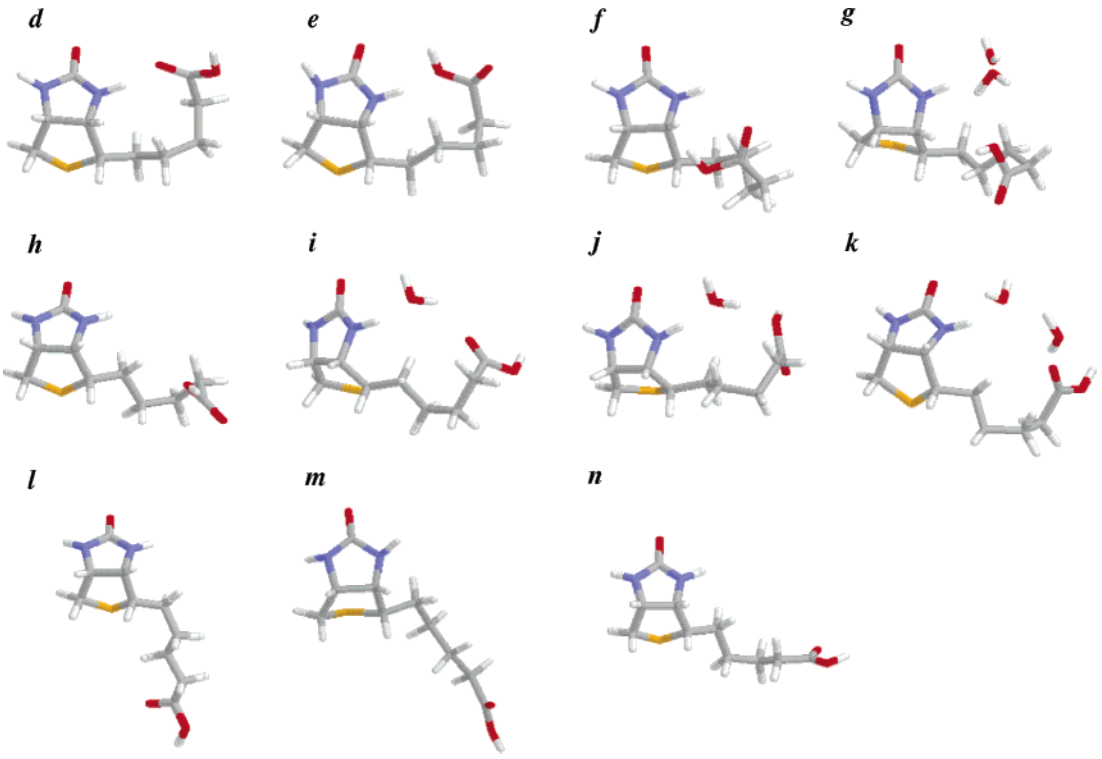

Figure 4. Three classes of conformations and average conformation obtained during dynamics of biotin in aqueous solution. ***d***, representative example of folded with N3−H3···O1′ intramolecular H-bond. ***e***, folded with N3−H3···OH intramolecular H-bond. ***f***, folded without intramolecular H-bond. ***g***, folded with H3···$(H_2O)_2$···OH H-bonds. ***h***, semifolded without water-mediated H-bonds. ***i***, semifolded with H3···(H_2O)···O1′ H-bonds. ***j***, semifolded with H3···(H_2O)···OH H-bonds. ***k***, semifolded with H3···$(H_2O)_2$···O1′ H-bonds. ***l***, extended similar to that of biotin in crystal. ***m***, extended similar to that of biotin bound to proteins. ***n***, average conformation.

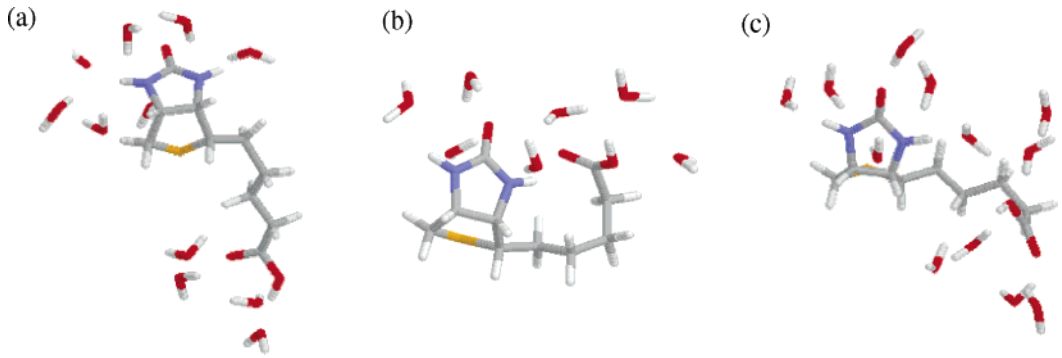

Figure 5. Representative hydrated structures of (a) extended, (b) folded, and (c) semifolded biotin showing the nearest water solvation shell within 2.4 Å of any biotin atom.

of hydration. The example in Figure 5a indicates that there are 11 closest water molecules within 2.4 Å of any biotin atom. As anticipated, the ureido and carboxyl groups form a number of hydrogen bonds with water molecules. The plentiful intermolecular hydrogen bonds to water play a dominant role to disrupt the intramolecularly hydrogen bonded states of biotin.

The net energetic gain associated with intramolecular hydrogen bonding formation must compete with various factors that oppose hydrogen bonded ring closure. First, the hydrogen bonding enthalpy is sufficient to overcome a certain amount of torsional strain and long-range nonbonded repulsion. However, the hydrogen bonding enthalpy cannot offset the energetic cost of even small distortions in covalent bond lengths or angles. Second, the loss of conformational freedom should lead to an increasing entropic barrier. When an intramolecular hydrogen bond forms, the motion of carbon−carbon single bond in the methylene groups of the side chain must be restricted. Therefore, the most enthalpically favorable intramolecularly hydrogen bonded geometries are entropically disfavored. Third, the hydrogen bonding capacity of the solvent will affect the conformation-directing role of intramolecular hydrogen bond. If the solvent forms strong hydrogen bonds with the solute, the enthalpic gain from the formation of intramolecular hydrogen bond will be severely diminished or abolished. Klotz and Franzen found that hydrogen bonding solvents such as dioxane and water could disrupt intramolecular amide−amide hydrogen bonding. They also found that the hydrogen bonding capacity of the solvent exerted the dominant influence on intramolecular amide−amide hydrogen bond.[29]

Conformers ***b*** and ***c*** are the low energy structures in vacuo, where the conformation of biotin is severely affected by intramolecular Coulombic repulsion or attraction and intramolecular hydrogen bonding formation. However, this situation may be radically different in water. The intramolecularly hydrogen bonded states disappear immediately when they are placed in water, which implies that the cyclically hydrogen bonded states are favored by the enthalpic gain associated with the formation of the intermolecular hydrogen bond. As described

TABLE 3: Probabilities (%) and Lengths of Hydrogen Bonding Formation (Å) between the Ureido Group and Water Molecules

	average		folded and semifolded		extended	
H-bond	probability	bond length	probability	bond length	probability	bond length
H1···OW	95.5	1.875	94.9	1.874	95.6	1.876
N1···HW	71.9	2.017	69.6	2.023	72.6	2.014
H3···OW	91.8	1.895	79.5	1.903	95.2	1.892
N3···HW	63.1	2.068	62.3	2.059	63.5	2.072

in the previous section, the graphical inspection has indicated that the side chains do form a few intramolecularly hydrogen bonded conformations, but they are mostly exposed to solvent water in the course of 15-ns simulation trajectory. Especially interestingly, the graphical inspection further observes many water bridges between the ureido group and the carboxyl group of the side chain by hydrogen bonding interaction, approximately corresponding to distances of H3···O1′ or H3···OH in the region of 4.0−5.5 Å, such as for the conformations of ***g***, ***i***, ***j***, and ***k*** shown in Figure 4. They are also found to be the transition structures of the intramolecularly hydrogen bonded states. The simulations reveal that even though the folded conformations of a 10-membered ring can tolerate N−H···O intramolecular hydrogen bond angles which approach linearity, the semifolded conformations of 13-membered and 16-membered rings will accommodate geometrically more favorable hydrogen bonding donor−acceptor orientations, smaller torsional and nonbonded strains, and less distortions in covalent bond lengths or angles in the linking segment. Therefore, the side chain exerts an influence on the ureido group mainly by the transfer of water molecules.

Comparison to NMR Experiments. The X-ray experiment showed an extended conformation of solid states of free and protein-bound biotin. In contrast, NMR studies suggested a more compact structure of biotin in the aqueous solutions.[10,12] The folded conformations with the intramolecular hydrogen bonds were introduced to interpret the difference between the 1-NH and 3-NH groups in the aqueous solutions. Unfortunately, NMR could not provide a direct measurement of the intramolecularly hydrogen bonded "folding". Our simulations confirm the speculation that biotin will satisfy its tendency to fold via the intramolecular hydrogen bonds. These folded states only happen at a few fractions during the 15-ns simulation. Although the folded conformations can generate the NOE signals and steric hindrance, the more favored semifolded conformations are responsible for the effects.

The probability distributions of R_g^2 in the 15-ns simulation are displayed in Figure 6, indicating that there exist quite a few folded and semifolded conformations. As a result of folding and semifolding, the side chain reduces the accessibility of the 3-NH. The steric hindrance of the side chain seems responsible for the difference between the 1-NH and 3-NH. However, it is important to point out that the side chain also greatly increases the hydrogen bonding capability of the 1-NH on the basis of the NMR data.[10−12,16] Therefore, it is not appropriate to attribute the difference to slowing down the 3-NH exchange rate due to the steric hindrance. Instead, speeding up the 1-NH exchange should be attributed to a certain effect of the side chain. Furthermore, it has turned out that biotin without the carbonyl group of the ureido part is inactive. The first step of enzymatic carboxylation entails the carboxylation of biotin by nucleophilic attack of nitrogen atom of the ureido group at bicarbonate. However, the nucleophilicity of nitrogen atom is very poor, hence an activation of the 1-NH site would have to take place during the enzymatic process.

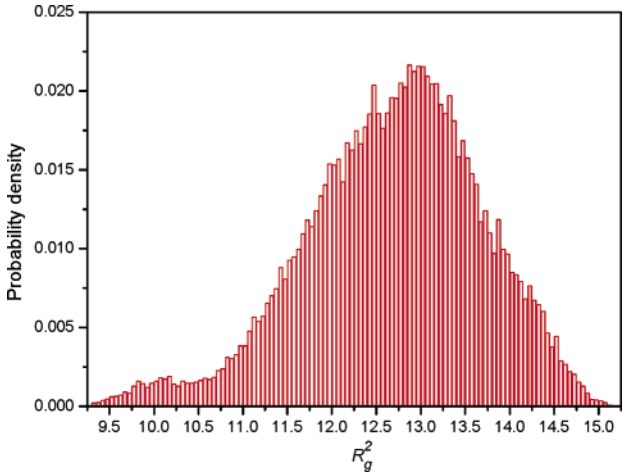

Figure 6. Probability distribution of the square of the radius of gyration (R_g^2) for biotin in aqueous solution in the 15-ns simulation trajectories. Bins correspond to 0.05 Å intervals.

Hydrogen Bonding Cooperativity. To answer the aforementioned third question, we further investigate the interactions of the NH groups and water molecules by radial distribution functions [$g(r)$'s] and statistics of hydrogen bonds shown in Figure 7a and Table 3, respectively. The $g(r)$'s, the average probabilities, and lengths of hydrogen bonding formation all indicate that the H1 site possesses stronger hydrogen bonding capability than the H3. The simulation results are qualitatively consistent with the experimental data. When the side chain folds or semifolds to be close to the ureido ring, the carboxyl and ureido groups will gather round to be a greater hydrophilic center and to form the hydrogen bonding network of biotin and a lot of water molecules. Two such representative clusters are displayed in Figure 5b,c, where the cooperativity is likely to appear in the hydrogen bonding networks. To better understand the effect of the side chain, we choose two segments of trajectories from simulation 1 for comparison, which are shown in Figure 7b,c. One is that of the folded and semifolded conformations, and the other is that of the extended ones. The hydrogen bonding capabilities of the two types of the NH groups are characterized in Table 3. The H3 site of the folded and semifolded conformations exhibits a little higher first peak than that of the extended in the $g(r)$'s. However, the H1 site of the folded and semifolded conformations represents much stronger hydration than that of the extended. The hydrogen bonds with water molecules will activate the 1-NH proton. As described in previous studies,[30−38] once the 3-NH forms hydrogen bonds, the hydrogen bonding capability of the H1 site could be increased. Interactions of this type have been referred to as hydrogen bond cooperativity.[30,31] Then the cooperativity will increase the N−H bond length while causing a greater reduction in the NH···OW distances, which further activates the 1-NH protons and facilitates the electrophilic substitution of the 1-NH. In our simulations, the H3 site of the folded and semifolded conformations represents the lower probability of hydrogen bonding formation and longer H3···OW distance than those of

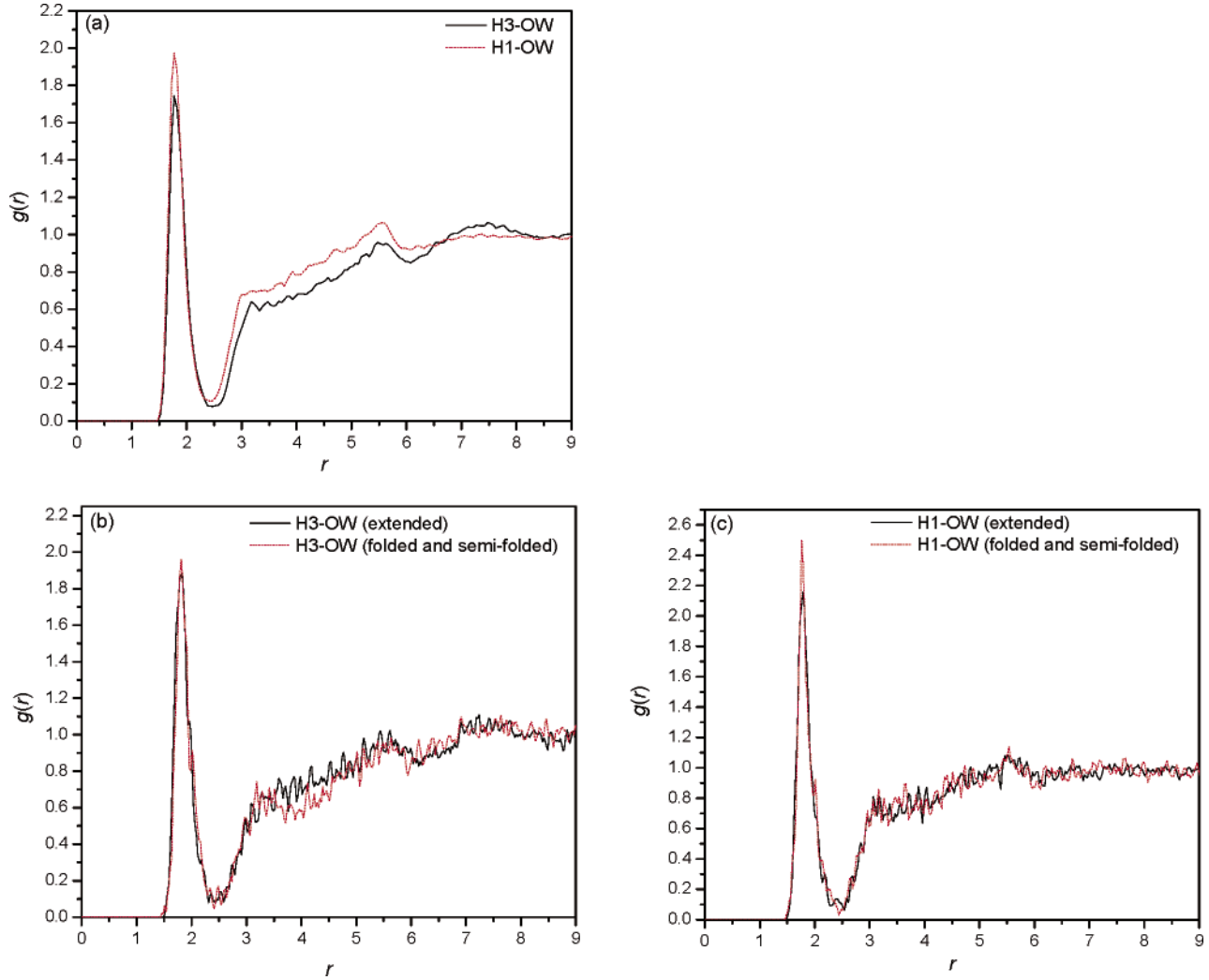

Figure 7. $g(r)$'s (in Å) of water molecules centered on the two NH sites of biotin. (a) $g(r)$[H3−OW] and $g(r)$[H1−OW]. (b) $g(r)$[H3−OW] of the folded and semifolded and $g(r)$[H3−OW] of the extended. (c) $g(r)$[H1−OW] of the folded and semifolded and $g(r)$[H1−OW] of the extended. The atom types refer to those in Table 1.

the extended, but those of the H1 site hardly change. It must be remembered that in most molecular mechanics force fields a hydrogen bond is described purely as an electrostatic attraction, with no charge transfer component. Also, the rigid and nonpolarizable pair potentials are employed in the OPLS all atom and SPC models. Thus, it could be understood that obvious cooperativity is not observed in the simulation. In the urea chain system, Masunov and Dannenberg et al. also used ab initio quantum chemical calculations to find the hydrogen bonding cooperativity that the last hydrogen bond became increasingly strong as the chain of urea grew.[34] Similarly, we speculate the folded and semifolded states in aqueous solution are a probable way of activating the 1-NH by this cooperativity. It is becoming increasingly apparent that nonadditive cooperative interaction plays an important role in hydrogen bonding interactions. To gain a deeper insight into the hydrogen bonding cooperativity of biotin, a quantum mechanical calculation should be further performed.

4. Conclusions

MD simulations have been employed to study the conformational properties and dynamics of biotin in aqueous solution for the first time, which gains an insight into the nature of the biotin solution structure by providing data complementary to the existing experimental data. In this paper, we mainly answer the three questions presented in the above paragraphs. Biotin in aqueous solution is not unique, but instead there will be an equilibrium distribution among different conformations. The average structure in aqueous solution appears to be an extended conformation, which is a little more compact than those of free or protein-bound biotin molecules in the crystal structures. The simulations confirm the folded conformations with the intramolecular hydrogen bonds, and further observe many semifolded conformations involving water-mediated hydrogen bonds between the ureido group and the carboxyl group of the side chain. Although the folded states happen at a few fractions during the 15-ns simulation, they could be important to the biological significance of biotin. While the hydrophilic carboxyl group of biotin approaches the other hydrophilic ureido group via folding over on itself, water molecules will gather round to form the hydrogen bonding network which is likely to induce the hydrogen bonding cooperativity. The cooperative effect will activate the 1-NH protons so that the 1-NH group can be deprotonated more easily by suitable groups of the enzyme in its vicinity. This behavior is exactly what one would expect when there is a switch to control the enzymatic process. We conclude that the side chain, conformational flexibility, water molecules, and hydrogen bonding cooperativity may play an essential role in activation of the 1-NH site toward carboxylation in the first step of biotin-dependent CO_2 transfer.

In view of the defect of classical force field, further work is required to carry out a high-level quantum chemical calculation to investigate the cooperativity of biotin in detail.

Acknowledgment. We are grateful to Prof. W. L. Jorgensen of Yale University for providing the OPLS all atom force field of biotin. This work was supported by the National Natural Science Foundation of China (No. 29976035) and Zhejiang Provincial Natural Science Foundation of China (No. RC01051).

Supporting Information Available: Bond stretching, angle bending, and torsional potential parameters of biotin; time series for simulations 2 and 3. This material is available free of charge via the Internet at http://pubs.acs.org.

References and Notes

(1) Lehninger, A. L.; Nelson, D. L.; Cox, M. M. *Principles of Biochemistry*, 2nd ed.; Worth Publishers: New York, 1993.

(2) Knowles, J. R. *Annu. Rev. Biochem.* **1989**, *58*, 195.

(3) Jitrapakdee, S.; Wallace, J. C. *Biochem. J.* **1999**, *340*, 1.

(4) Attwood, P. V. *Int. J. Biochem. Cell Biol.* **1995**, *27*, 231−249.

(5) Chilkoti, A.; Stayton, P. S. *J. Am. Chem. Soc.* **1995**, *117*, 10622.

(6) Weber, P. C.; Ohlendorf, D. H.; Wendoloski, J. J.; Salemme, F. R. *Science* **1989**, *243*, 85.

(7) (a) Diamandis, E. P.; Christopoulos, T. K. In *Immunoassay*; Diamandis, E. P., Christopoulos, T. K., Eds.; Academic Press: San Diego, 1996. (b) Deshpande, S. S. *Enzyme Immunoassays: From Concept to Product Development*; Chapman & Hall: New York, 1996. (c) Wild, D. In *The Immunoassay Handbook*; Wild, D., Ed.; Stockton Press: New York, 1994.

(8) McClain, K. L.; Baker, H.; Onstad, G. R. *J. Am. Med. Assoc.* **1982**, *247*, 3116.

(9) (a) Pugliese, L.; Coda, A.; Malcovati, M.; Bolognesi, M. *J. Mol. Biol.* **1993**, *231*, 698. (b) Hyre, D. E.; Le Trong, I.; Freitag, S.; Stenkamp, R. E.; Stayton, P. S. *Protein Sci.* **2000**, *9*, 878.

(10) Fry, D. C.; Fox, T. L.; Lane, M. D.; Mildvan, A. S. *J. Am. Chem. Soc.* **1985**, *107*, 7659.

(11) Perrin, C. L.; Dwyer, T. J. *J. Am. Chem. Soc.* **1987**, *109*, 5163.

(12) Tonan, K.; Adachi, K.; Ikawa, S. *Spectrochim. Acta, Part A* **1998**, *54*, 989.

(13) Gellman, S. H.; Dado, G. P.; Liang, G.-B.; Adams, B. R. *J. Am. Chem. Soc.* **1991**, *113*, 1164.

(14) Diaz, H.; Espina, J. R.; Kelly, J. W. *J. Am. Chem. Soc.* **1992**, *114*, 8316.

(15) Tsang, K. Y.; Diaz, H.; Graciani, N.; Kelly, J. W. *J. Am. Chem. Soc.* **1994**, *116*, 3988.

(16) Crisp, G. T.; Jiang, Y. L. *ARKIVOC* **2001**, *7*, 77.

(17) (a) Goodall, G. J.; Baldwin, G. S.; Wallace, J. C.; Keech, D. B. *Biochem. J.* **1981**, *199*, 603. (b) Attwood, P. V.; Wallace, J. C. *Biochem. J.* **1986**, *235*, 359. (c) Werneburg, B. G.; Ash, D. *Biochemistry* **1997**, *36*, 14392.

(18) Sanchez, E. R.; Gessel, M. C.; Groy, T. L.; Caudle, M. T. *J. Am. Chem. Soc.* **2002**, *124*, 1933.

(19) Strzelczyk, A. A.; Dobrowolski, J. C.; Mazurek, A. P. *J. Mol. Struct. (THEOCHEM)* **2001**, *541*, 283.

(20) (a) Jorgensen, W. L.; Maxwell, D. S.; Tirado-Rives, J. *J. Am. Chem. Soc.* **1996**, *118*, 11225. (b) McDonald, N. A.; Jorgensen, W. J. *J. Phys. Chem. B* **1998**, *102*, 8049.

(21) Berendsen, H. J. C.; Postma, J. P. M.; van Gunsteren, W. F.; Hermans, J. In *Intermolecular Forces*; Pullman, B., Ed.; Reidel: Dordrecht, 1981; pp 331−342.

(22) Dudek, M. J.; Ramnarayan, K.; Ponder, J. W. *J. Comput. Chem.* **1998**, *19*, 548. See also http://dasher.wustl.edu/tinker.

(23) Berendsen, H. J. C.; Postma, J. P. M.; Van Gunsteren, W. F. *J. Chem. Phys.* **1984**, *81*, 3684.

(24) Brooks, B. R. In *Algorithms for Molecular Dynamics at Constant Temperature and Pressure*; DCRT Report; NIH, April 1988.

(25) Toukmaji, A. Y.; Board, J. A., Jr. *Comput. Phys. Commun.* **1996**, *95*, 73.

(26) Andersen, H. C. *J. Comput. Phys.* **1983**, *52*, 24.

(27) Lei, Y.; Li, H.; Pan, H.; Han, S. *J. Phys. Chem. A* **2003**, *107*, 1574.

(28) Connolly, M. L. *J. Appl. Crystallogr.* **1983**, *16*, 548.

(29) Klotz, I. M.; Franzen, J. S. *J. Am. Chem. Soc.* **1962**, *84*, 3461.

(30) Karpfen, A. *Adv. Chem. Phys.* **2002**, *123*, 469.

(31) Scheiner, S. *Hydrogen Bonding: A Theoretical Perspective*; Oxford University Press: New York, 1997.

(32) Ludwig, R.; Reis, O.; Winter, R.; Weinhold, F.; Farrar, T. C. *J. Phys. Chem. B* **1998**, *102*, 9312.

(33) Ludwig, R. *Phys. Chem. Chem. Phys.* **2002**, *4*, 5481.

(34) Masunov, A.; Dannenberg, J. J. *J. Phys. Chem. B* **2000**, *104*, 806.

(35) Kobko, N.; Paraskevas, L.; del Rio, E.; Dannenberg, J. J. *J. Am. Chem. Soc.* **2001**, *123*, 4348.

(36) Guo, H.; Gresh, N.; Roques, B. P.; Salahub, D. R. *J. Phys. Chem. B* **2000**, *104*, 9746.

(37) Klein, R. A. *J. Am. Chem. Soc.* **2002**, *124*, 13931.

(38) Parra, R. D.; Bulusu, S.; Zheng, X. C. *J. Chem. Phys.* **2003**, *115*, 3499.